Limnologica 68 (2018) 142–156

Contents lists available at ScienceDirect

Limnologica

journal homepage: www.elsevier.com/locate/limno

Shallow bedrock limits groundwater seepage-based headwater climate refugia

Martin A. Briggs[a,*], John W. Lane[a], Craig D. Snyder[b], Eric A. White[a], Zachary C. Johnson[b], David L. Nelms[c], Nathaniel P. Hitt[b]

[a] U.S. Geological Survey, Office of Groundwater, Branch of Geophysics, 11 Sherman Place, Unit 5015, Storrs, CT 06269, USA
[b] U.S. Geological Survey, Leetown Science Center,11649 Leetown Road, Kearneysville, WV 25430, USA
[c] U.S. Geological Survey, Virginia Water Science Center,1730 East Parham Road, Richmond, VA 23228, USA

ARTICLE INFO

Article history:
Received 26 May 2016
Received in revised form 15 February 2017
Accepted 21 February 2017
Available online 6 March 2017

Keywords:
Groundwater/surface water
Hydrological exchange
Trout
Refugia
Climate
Geophysical
Hyporheic
Climate change
Heat tracer
Headwater

ABSTRACT

Groundwater/surface-water exchanges in streams are inexorably linked to adjacent aquifer dynamics. As surface-water temperatures continue to increase with climate warming, refugia created by groundwater connectivity is expected to enable cold water fish species to survive. The shallow alluvial aquifers that source groundwater seepage to headwater streams, however, may also be sensitive to seasonal and long-term air temperature dynamics. Depth to bedrock can directly influence shallow aquifer flow and thermal sensitivity, but is typically ill-defined along the stream corridor in steep mountain catchments. We employ rapid, cost-effective passive seismic measurements to evaluate the variable thickness of the shallow colluvial and alluvial aquifer sediments along a headwater stream supporting cold water-dependent brook trout (*Salvelinus fontinalis*) in Shenandoah National Park, VA, USA. Using a mean depth to bedrock of 2.6 m, numerical models predicted strong sensitivity of shallow aquifer temperature to the downward propagation of surface heat. The annual temperature dynamics (annual signal amplitude attenuation and phase shift) of potential seepage sourced from the shallow modeled aquifer were compared to several years of paired observed stream and air temperature records. Annual stream water temperature patterns were found to lag local air temperature by ~8–19 d along the stream corridor, indicating that thermal exchange between the stream and shallow groundwater is spatially variable. Locations with greater annual signal phase lag were also associated with locally increased amplitude attenuation, further suggestion of year-round buffering of channel water temperature by groundwater seepage. Numerical models of shallow groundwater temperature that incorporate regional expected climate warming trends indicate that the summer cooling capacity of this groundwater seepage will be reduced over time, and lower-elevation stream sections may no longer serve as larger-scale climate refugia for cold water fish species, even with strong groundwater discharge.

Published by Elsevier GmbH.

1. Introduction

Streams, lakes, and shallow aquifers are warming worldwide (Eggleston and McCoy, 2015; Isaak et al., 2012; O'Reilly et al., 2015). This warming will increasingly stress thermally sensitive aquatic species such as salmonid fishes, particularly during spring and summer months (Isaak et al., 2015, 2012; Kanno et al., 2016; Meisner, 1990). Mountain headwater streams may exhibit reduced warming rates and "climate velocities" (Isaak et al., 2016), but the resilience and connectivity of these cold water habitats is likely to be controlled in part by local groundwater (GW) flowpath characteristics, which are typically not well defined. Focused GW seepage to surface water (SW) generates thermal discontinuities in stream temperature in response to localized conductive and advective heat exchange (Caissie et al., 2014), creating isolated zones of thermal refugia when the prevailing surface-water condition exceeds thermal tolerance thresholds (Ebersole et al., 2003; Mathews and Berg, 1997). More contiguous reach-scale climate refugia are formed when GW influence preserves cold water habitat against long-term air temperature warming (Isaak et al., 2015). In addition to reducing summer surface-water temperatures, GW seepage acts to reduce short-term thermal variability (e.g. diurnal) due to the buffering influence of heat exchange with SW, which may also impact the survival of stressed organisms (Briggs et al., 2013).

* Corresponding author.
E-mail address: mbriggs@usgs.gov (M.A. Briggs).

https://doi.org/10.1016/j.limno.2017.02.005
0075-9511/Published by Elsevier GmbH.

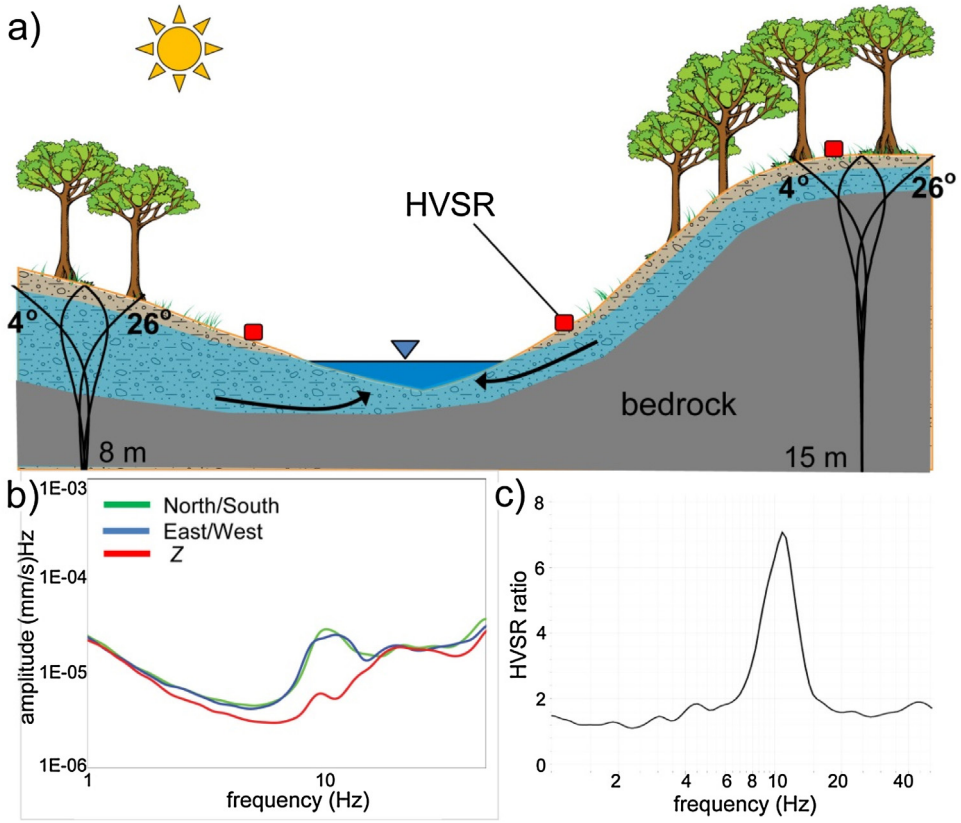

Fig. 1. (Panel a) shows the control varied depth to low-permeability bedrock can exert on shallow groundwater flow, and subsequently, seepage temperature stability; temperature/depth profiles extracted from the "climate warming" numerical model every 3 months are used to create the idealized annual temperature envelopes. Surface HVSR seismic measurements are used to evaluate unconsolidated aquifer thickness in transects through the riparian zone. (Panel b) displays example ambient seismic information collected in 3 directions, which is analyzed for the resonance frequency (peaks) shown in the final HVSR curve (panel d), which is converted to bedrock contact depth using the measured shear wave velocity (mean = 346 ms^{1}).

Thermal influence from GW also enables various heat tracing methodologies that locate anomalously buffered (Rosenberry et al., 2016b) or cooled (e.g. Dugdale et al., 2015) zones to map potential thermal refugia in rivers. Through the collection of collocated air and water thermal time series, the sensitivity of SW temperature to local air temperature change (typically daily or weekly variation) can be evaluated with a variety of linear regression techniques (Kelleher et al., 2012; Snyder et al., 2015). Locations with relatively low sensitivity to air temperature change along a stream network may indicate zones of GW influence. Empirical sensitivity analyses such as these lend important insight into stream habitat fragmentation and resilience to climate warming (Snyder et al., 2015). Hyporheic exchange with coarse alluvium may also reduce short-term temperature variation (Johnson, 2004), moderating the minimum and maximum diurnal swings (Arrigoni et al., 2008), but hyporheic exchange is not expected to greatly moderate the longer-term annual stream temperature signal in the absence of GW seepage. Previous work has indicated stream and air annual signals are expected to essentially be in-phase along streams of varied size and position within the network (Caissie et al., 2005), though this assumes GW seepage functions only as a buffer and does not impart a temporally variable thermal signal on stream water.

Despite the usefulness of linear regression-based stream temperature sensitivity techniques, they offer limited understanding regarding the characteristics of GW flowpaths that sustain seepage zones, including the sensitivity of such flowpaths to annual air temperature patterns (Kurylyk et al., 2015). Although GW temperature at any time of year is often approximated by the local mean air temperature (Constantz, 2008), this estimate is inherently based on an assumption that the GW flow path in question travels below the "thermal envelope" of annual temperature variation (Fig. 3 in Stonestrom and Constantz, 2003). When the depth of GW flow within the upper unconfined alluvial aquifer is constrained within the annual envelope, by definition, the water will be sensitive to annual surface temperature dynamics and display annual thermal variation (Fig. 1a), regardless of water age/residence time. Kurylyk et al. (2014) found that the degree of damping of the annual signal in GW seepage zones was strongly tied to the depth of a confining till layer below the shallow aquifer indicating that shallow aquifers (e.g., <10 m depth) will show less short-term resilience to climate warming.

Native brook trout (*Salvelinus fontinalis*) in eastern North America are commonly associated with GW fed systems (MacCrimmon and Campbell, 1969), as indicated by the Latin word *fontinalis*, which can be translated to "of spring". Brook trout exhibit an upper lethal temperature limit of approximately 25 °C (Fry et al., 1946) and typically do not occur where 60-d mean temperatures exceed 21 °C, or when maximum weekly average summer stream temperature (*MWAT*) exceeds 23.3 °C (Wehrly et al., 2007). Habitat loss and degradation has substantially reduced brook trout abundance and distribution across much of their native range, particularly in valley areas (Hudy et al., 2008). Consequently, brook trout are often restricted to high elevation forested mountain streams throughout much of their native range.

In mountain watersheds, GW sources are typically associated with shallow aquifers of mixed alluvium and colluvium that are commonly constrained vertically by shallow bedrock (e.g., Fig. 31 in Nelms and Moberg, 2010), and GW seepage to streams is strongly tied to nearby hillslope dynamics (Bergstrom et al., 2016; Jencso

et al., 2010). Thus, stream water may exhibit strong bidirectional exchange with these permeable sediments forming a mosaic of losing and gaining zones throughout the drainage network (Payn et al., 2009). This connectivity from GW to SW can serve to cool streams in summer and buffer short-term air temperature swings (Hare et al., 2015), but the underlying confinement by shallow bedrock may compromise montane alluvial GW contribution to thermal and climate refugia. Unfortunately, it is difficult and expensive to collect sediment cores and auger wells in steep, rocky terrain, so distributed information regarding bedrock depth, and hence climate sensitivity, is typically not available.

Geophysical methods utilizing passive and active signals (e.g., geoelectrical, radar) to characterize the subsurface are progressively being applied to hydrologic research (Binley et al., 2015). However, these tools may not be appropriate in some mountain stream settings where equipment transportation and field deployment is challenging. For instance, acquisition and analysis of electrical measurements in the stream corridor is complicated by rugged topography and abundant near-surface cobbles; furthermore, electrical methods are sensitive to variations in saturation, water salinity and the underlying geology, parameters that are often strongly heterogeneous in streambed settings (Ward et al., 2010). Similarly, ground penetrating radar surveys in mountain stream settings can be hindered by poor antenna coupling in rugose streams, and the interpretation of reflection profiles to identify the bedrock surface complicated by diffractions from cobble-type materials, potentially reducing accuracy and precision.

The horizontal-to-vertical spectral ratio (HVSR) method is a passive geophysical technique that utilizes three-component measurements of ambient seismic noise to identify and assess seismic resonance. HVSR was popularized by Nakamura (1989) in the context of seismic hazard assessment and is widely used in Europe and Japan (see Mucciarelli and Gallipoli, 2001; Bonnefoy-Claudet et al., 2006, for reviews). The HVSR method is frequently used as a geophysical exploration tool to estimate sediment thicknesses in the 10^1–10^3 meter range (e.g. Delgado et al., 2000; Parolai et al., 2002; Yanamaka et al., 1994) and is increasingly used in the United States in support of GW availability and contaminated site investigations (e.g. Campbell and Landmeyer, 2014; Fairchild et al., 2013; Lane et al., 2008). However, the HVSR method has not been well-evaluated for the quantification of thin sediment thicknesses (e.g. <5 m depth), such as might be expected throughout the stream corridor in steep mountain watersheds, or to our knowledge ever applied specifically to GW-SW exchange research. We hypothesize that HVSR may be a cost effective and robust addition to existing geophysical tools capable of estimating sediment thickness to inform inferences regarding climate sensitivity and GW influence.

Locating present-day cold anomalies in streams during summer is insufficient to estimate stream thermal responses to climate change. Given the growing recognition of the strong relation between stream climate refugia and GW seepage, adjacent GW flow-path dynamics need to be defined to more reliably inform process-based management of cold water fish species in a warming climate. We use a steep mountain watershed supporting brook trout in Shenandoah National Park, VA, USA (SNP), and GW seepage influence to investigate the following research questions:

1. Does the depth to bedrock vary throughout the stream corridor, and how might this vertical constraint affect the propagation of present-day surface temperature dynamics into the shallow aquifer and through seepage zones?
2. How sensitive is GW seepage to predicted decadal air temperature warming within native brook trout habitat in the Chesapeake Bay watershed (where the Shenandoah National Park is located)?

2. Methods

A combination of long-term daily temperature records and HVSR depth to bedrock measurements were used to parametrize one-dimensional (1D) models of shallow aquifer vertical heat transport.

2.1. Site description

The SNP is 80,000 ha of predominantly forested land in the Blue Ridge Mountains of northern VA, USA, with well characterized hydrogeology and stream ecology (Busenberg et al., 2014; DeKay, 1972; Plummer et al., 2001). Steep headwater basins range in elevation from 168 m to 1125 m, with the total stream length dominated (92%) by first, second, and third-order channels (Snyder et al., 2013). GW seepage from unconsolidated, shallow alluvium and colluvium aquifers sustain perennial streams through periods of low flow (e.g., Fig. 31 in Nelms and Moberg, 2010), which typically correspond to periods of warm air temperature (DeKay, 1972; Snyder et al., 2013). Due to the low permeability of basaltic and granitic bedrock that underlies much of the central and northern SNP ridgeline, deep fracture flow is thought to be a minor contribution to streamflow, although fracture flow may sustain isolated hillslope perennial springs (Nelms and Moberg, 2010). Focused GW discharge points throughout SNP were extensively surveyed for spatiotemporal temperature dynamics in the late 1990s (Plummer et al., 2001) and indicated variable sensitivity to seasonal air temperature with mean temperatures generally related to elevation.

Long-term (in-situ) headwater stream temperature records are generally sparse (Isaak et al., 2016), but from 2012 to present at least 81 stream locations throughout 9 watersheds in SNP have been monitored for hourly temperature using HOBO Pro V2 thermographs with 0.2 °C accuracy and drift = <0.1 °C per year (Onset Computer Corp., Cape Cod, USA); many points have a collocated air temperature logger (Snyder et al., 2015). Combined stream and air data have been used to assess local channel sensitivity to short-term summer air temperature variation (e.g., seasonal and diurnal signals, storms) and linear models have been used to develop metrics of "GW influence", assuming that strong advective and conductive heat exchanges in seepage zones function to decouple air and water thermal time series compared to non-seepage zones (Snyder et al., 2015). The multi-year paired air and water data had not been analyzed for longer-term annual temperature signal dynamics.

Whiteoak Canyon (WOC) was chosen as a case study example for this analysis (Fig. 2a and b) due to the observed large range in apparent GW seepage influence (Snyder et al., 2015), diverse morphology, and the existence of a previously drilled riparian well providing known bedrock depth that could be used in method (HVSR) validation. The watershed has zones of brook trout habitat split between upper (~950–1050 m) and lower (~350–450 m) stream segments that are separated by a steep zone dominated by large waterfalls (Fig. 2a). The stream initiation point from the porous alluvium/colluvium of the upper valley has been observed to shift vertically depending on the time of year and antecedent precipitation conditions. The upper section, approximately 1 km below the general initiation point, was characterized by Snyder et al. (2015) as having some of the strongest GW influence in SNP, while the lower section had reduced GW buffering of diurnal temperature swings. Median focused spring temperature across SNP averaged 8.5 °C for elevations corresponding to the upper section, and 11.5 °C for the lower section, respectively, though a relatively large range was observed (Busenberg et al., 2014; Table 1).

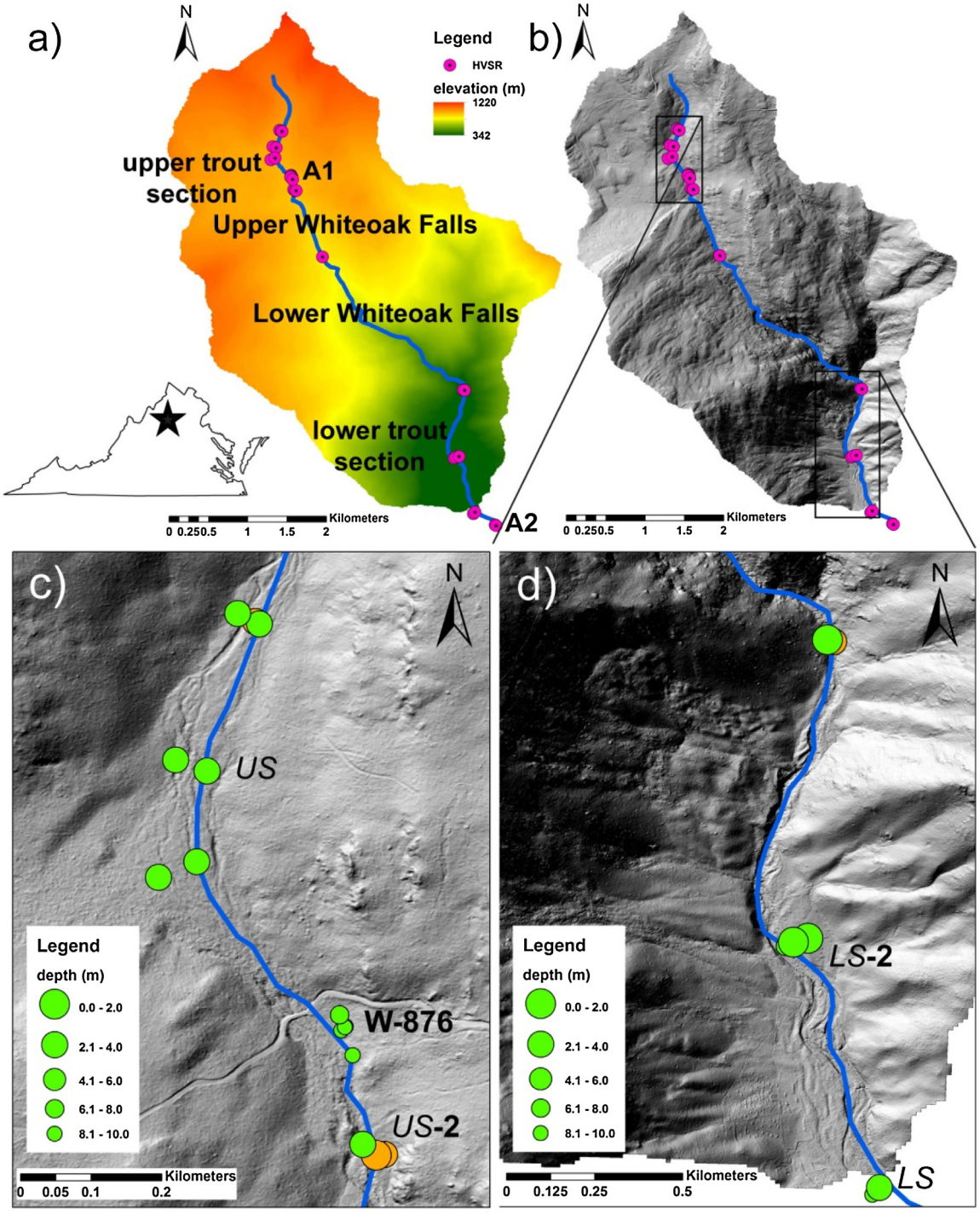

Fig. 2. The Whiteoak Canyon watershed, located in Shenandoah National Park, within the larger Chesapeake Bay watershed, drains to the south over approximately 900 m of elevation. (Panel a) displays the general elevation change and locations of the upper and lower trout habitat sections and HVSR measurement locations. When a hillshade function is applied to the elevation data (panel b) the steep, variable terrain of the watershed can be better visualized. (Panels c and d) display depth to bedrock data as evaluated with HVSR measurement for the upper and lower trout sections, respectively; orange colored dots indicate a more poorly coupled HVSR measurement (rating of "3"). The riparian borehole area is indicated by "W-876", and captures a deeper alluvial sediment thickness (mean = 8.5 m) than was observed elsewhere along the stream (mean = 2.6 m). Vertical aquifer temperature dynamics were modeled numerically at the main upper stream (*US*) and lower stream (*LS*) trout habitat transects, and long-term paired air and water annual signals were compared to nearby stream transects (*US*-2, *LS*-2). (For interpretation of the references to colour in this figure legend, the reader is referred to the web version of this article.)

2.2. Seismic geophysical measurements

In September and December 2015, HVSR measurements were acquired at over 50 stations within WOC using Micromed Model TEP-3C seismometers; the fundamental theory of the measurements is explained here. Usually, a 10-min ambient-noise measurement is sufficient to assess bedrock interfaces at depths less than 25 m. The method requires a measurement or estimate of shear wave velocity (V_S), which depends on sediment composition, for the conversion of measured resonance frequency to a depth to bedrock. For sites that can be approximated as a two-layer model

Table 1
The basic temperature statistics of notable springs throughout Shenandoah National Park at elevations corresponding to the two approximate reaches of potential trout habitation in Whiteoak Canyon; data are compiled from Busenberg et al., 2014, originally collected 1995–2014.

elevation range (m)	Shenandoah National Park large spring water temperature statistics (°C)		
	low	median	high
350:450	8.1	11.5	16.0
950:1050	6.9	8.5	13.7

(Fig. 2a), the fundamental-mode seismic resonance frequency, f_r, is given by:

$$f_r = V_s/4Z \quad (1)$$

where V_s is the average shear-wave velocity (ms^{-1}) of the surficial materials and Z is the thickness of the surficial layer (m). In practice, f_r is determined from analysis of the spectral ratio of the horizontal [$S(\omega)_{NS}$ and $S(\omega)_{EW}$] and vertical [$S(\omega)_V$] components of the ambient seismic noise field, where ω is the angular frequency (e.g. Delgado et al., 2000; Nakamura, 1989):

$$HVSR(\omega) = \{[S^2(\omega)_{NS} + S^2(\omega)_{EW}]/2S^2(\omega)_V\}^{1/2} \quad (2)$$

Given f_r and V_s, Z is estimated using the relation shown in Eq. (1). As an alternative, some researchers correlate observed surficial layer thickness (e.g., from borings) and observed resonance frequency from HVSR data to develop empirical relations for depth estimation where V_s is unknown (e.g. Fairchild et al., 2013; Ibs-von Seht and Wohlenberg, 1999; Parolai et al., 2002). Here, we measure V_s experimentally using an active seismic technique (horizontal shear-wave seismic source recorded by a linear multi-channel seismic geophone array), then compare the application of this V_s to HVSR measurements collocated with a riparian well with known depth to bedrock along the upper section of WOC (Fig. 2C).

At each station, vegetative ground cover was removed, the instrument was oriented to magnetic north, coupled to the ground using short (~2 cm) spikes threaded into the base plate of the seismometer, and leveled. HVSR station locations were georeferenced using both hand-held and on-board global positioning system (GPS) receivers. Ambient seismic noise was recorded at a sampling frequency of 128 or 256 Hz for 10 min at each station (Fig. 2b). HVSR measurements were processed to determine f_r using a commercially available program (Grilla V6.1) and a freeware processing suite (Geopsy V2.7.0). Both programs compute the amplitude spectrum of the two horizontal and vertical components for each individual user-specified time-window (20 s for this study) (Fig. 1b), calculate the ratio of the average horizontal and vertical amplitude spectrums for each time-window, and determine the mean HVSR curve for the entire record (Fig. 1c).

2.3. Temperature measurements

Spatially discontinuous roving water surface and bank temperature surveys along the main channel were performed with a hand-held thermal infrared camera (FLIR T640bx, FLIR Systems Inc.). These reconnaissance surveys, collected in September and December 2015 were used to qualitatively assess the presence of seepage from deep GW flowpaths expected to approach 8 °C along the upper section (Table 1). We also installed vertical arrays of thermal data loggers to estimate bulk thermal diffusivity of the saturated alluvium at two stations in the upper trout section. The thermal parameters calculated from vertical diurnal signal propagation in the streambed were used in the numerical vertical aquifer models, described in Section 2.4 below. The vertical temperature profilers were composed of discrete thermal data loggers (0.0625 °C precision, iButton Thermochron DS1922L, Maxim Integrated) that were inserted into short slotted steel pipes at 0.01 and 0.07 m streambed depths (e.g. Rosenberry et al., 2016a). Loggers were set to record temperature at 1-h intervals between 12/04/2015 to 02/29/2016. Visual observations indicated the alluvium and colluvium material in WOC is highly permeable to flow, and a porosity of 0.4 was assumed, in accordance with similar material (McWhorter and Sunada, 1977). Although porosity does not need to be specified for the determination of saturated thermal diffusivity from diurnal signals, this unknown will affect the extrapolation of thermal properties to the unsaturated zone in the numerical models. We used methods proposed by Luce et al. (2013) and automated by the new VFLUX2 program (Irvine et al., 2015) to evaluate thermal diffusivity from the streambed temperature data. This approach simultaneously uses the amplitude reduction and phase-shift of the diurnal signal with depth to evaluate bulk thermal diffusivity of saturated porous media, irrespective of vertical flow rate.

The dynamic harmonic regression (DHR) routines of the Captain Toolbox program (Taylor et al., 2007) run by VFLUX2, typically applied to streambed diurnal signal analysis, were used to extract fundamental annual sinusoids from paired air and water time series. This was accomplished by resampling the hourly temperature data to 12–24 measurements per cycle (annual) as recommended for the DHR technique (Gordon et al., 2012), setting the "Pf" parameter of the main VFLUX2 routine to "365 d", and defining the fundamental harmonic signal of interest. The characteristics of extracted non-stationary annual sinusoids (phase, amplitude) from two locations in both the upper and lower reach main channel (Fig. 2c and d) were compared to local air sinusoids to explore signal attenuation and offset in time.

2.4. Numerical groundwater modeling

Variably saturated numerical models were developed to predict the temperature response of the shallow alluvial aquifer to seasonal air temperature variation in zones of current preferential brook trout habitation. GW seepage temperature to the stream will inherently reflect the aquifer from which seepage is derived. The downward transport of surface heat to shallow alluvial GW is influenced by: (1) vertical advective flow and infiltration, (2) bulk thermal diffusivity (conduction) of the aquifer, (3) unsaturated zone hydrodynamics and thickness, and (4) depth of flow-limiting bedrock. GW seepage to WOC sites is expected to originate from lateral and down-valley (including parafluvial) horizontal flow along the bedrock contact, with minimal vertical component. Shallow horizontal GW flow has been shown to have limited effect on the downward conduction of heat (Irvine et al., 2016; Vogt et al., 2012); therefore, lateral advection was neglected using a 1D numerical modeling strategy, similar to (Briggs et al., 2014), but vertical recharge infiltration is accounted for as described below.

Due to high apparent permeability of the alluvium (anticipated lack of GW mounding), the unsaturated zone thickness was approximated by the average (n = 10) incised stream channel depth to water, derived from light detection and ranging (lidar) data (NRCS, 2013; 76 cm cell size with 9.2 cm vertical resolution) and analyzed using ArcGIS software (Esri Inc., Redlands, CA). Finally, depth to bedrock was estimated using the HVSR method as described above. We use this depth to bedrock to constrain the "effective aquifer depth" from which seepage to the stream is sourced (Kurylyk et al., 2015). Although actual GW seepage to the stream will also be sourced from shallower depths within the saturated zone, the depth constraint imposed by bedrock allows us to explore the strongest expected attenuation of surface heating within these thin hillslope aquifers and therefore provides a conservative estimate of seepage thermal sensitivity.

Table 2
Thermo-physical characteristics of liquid, ice, and solid matrix used for numerical groundwater model simulations.

Ice Parameters	
Ice specific heat capacity ($J\,kg^{-1}\,C^{-1}$)	2108
Ice thermal conductivity ($Js^{-1}\,m^{-1}\,C^{-1}$)	2.14
Density of ice ($kg\,m^{-3}$)	920
Latent heat of fusion ($J\,kg^{-1}$)	334,000
Liquid Water Parameters	
Fluid specific heat capacity ($J\,kg^{-1}\,C^{-1}$)	4182
Fluid thermal conductivity ($Js^{-1}\,m^{-1}\,C^{-1}$)	0.6
Solid Matrix Parameters	
Solid grain specific heat capacity ($J\,kg^{-1}\,C^{-1}$)	898
Solid grain thermal conductivity ($Js^{-1}\,m^{-1}\,C^{-1}$)	2.9
Porosity	0.40

We developed transient 1D numerical simulations with a modified version of the SUTRA model (Voss and Provost, 2002) that accounts for variably saturated freeze-thaw dynamics (e.g. McKenzie and Voss, 2013) to predict annual alluvial aquifer temperature dynamics using coupled fluid and heat transport physics. Specified model thermal and sediment parameter values are listed in Table 2, including alluvium thermal parameters inferred from the streambed diurnal signal analysis described in Section 2.3. A bedrock layer was not included in the vertical aquifer models, so that annual thermal time series could be extracted at any depth of interest, and reasonably reflect expected temperature dynamics just above a bedrock contact.

Freeze-thaw processes were expected to have limited impact on the simulations given the temperate climate of Virginia, USA, so the simple linear functions of McKenzie and Voss (2013) were adopted here, including unsaturated zone water retention dynamics. Here vertical montane aquifer thermal dynamics were simulated with a columnar model domain that is 1 m wide, 1 m thick and spans +1 m to −20 m vertical depths relative to the ground surface. The near-surface model domain (0–5 m depths) consisted of 0.01 m vertical elements, while the lower domain (5–20 m) was parsed into 0.1 m vertical elements. A zero-pressure boundary was used to specify a constant water table depth at 1.4 m as indicated by the average stream channel incision depth to water. Daily recharge to the model domain was specified at the ground surface (0 m), and determined from monthly historical (1941–2016) precipitation data at the nearby Shenandoah National Park Service weather station (https://www.ncdc.noaa.gov/cdo-web/search; Luray 5 E, VA US, station number: GHCND:USC00445096); the zero-pressure boundary allowed water to exit the model and maintain a constant water table depth throughout the simulations. Recharge temperature was specified accordingly to average streamside monthly air temperature from years 2013 and 2015 as described below and indicated in Fig. 3.

The lower thermal boundary was specified to represent the geothermal gradient, similar to McKenzie and Voss (2013). Because of the large change in elevation of ~600 m between the upper and lower stream sections, the upper ground surface temperature was determined for each location separately using local streamside air temperature records collected in the manner detailed in Snyder et al. (2015). Streamside air temperature incorporates the effects of upper story vegetation (forest shading, evapotranspiration), and therefore the ground surface was assumed to be in equilibrium with this near-surface air. A 1 m thermal boundary layer (e.g. Mckenzie et al., 2007) with high thermal diffusivity was used to efficiently impart the seasonal signal onto the model domain at 0 m. This average seasonal thermal signal was determined by fitting a sinusoid (period 1 yr) to daily streamside air temperature data collected in 2013 and 2015 (2015 data were collected from 01/01/2015 to 09/15/2015 only), and these functions approximated

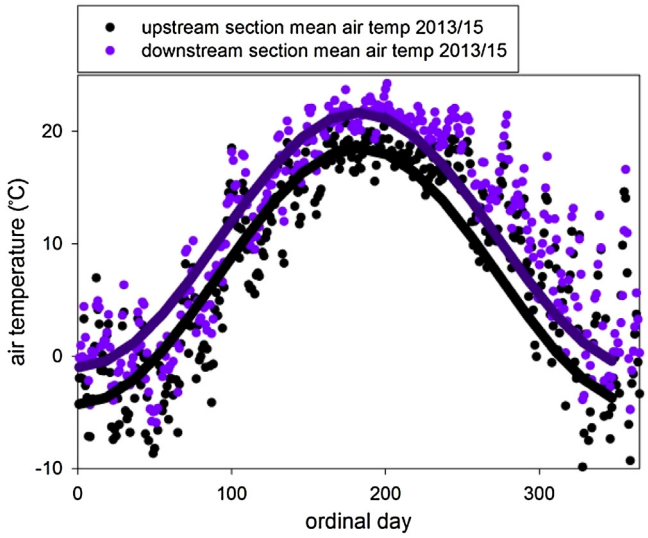

Fig. 3. Daily streamside air temperature, averaged between 2013 and 2015 for corresponding days, for the upper and lower trout stream sections. Sinusoids were used to approximate the yearly local measured air temperature dynamics for numerical modeling; maximum and minimum monthly air temperatures were used to define the sinusoid amplitude and mean.

average elevation-corrected historical values at the nearby Luray, VA, weather station. Streamside air temperature data were compiled to monthly averages, and the thermal boundary sinusoid mean was specified to reproduce observed minimum and maximum monthly values defining the amplitude of the annual signal. The phase of the annual model temperature sinusoid was shifted forward in time by 3 months (pi/2) to coincide with observed seasonal changes (Fig. 3). Finally, future (+75 yr) stream temperatures were predicted as described in Appendix A; expected regional climate warming of 5 °C/85 yr (Horton et al., 2014) was simulated for the "warming" numerical aquifer models by applying a linear trend to the upper boundary temperature sinusoid mean.

All models were run for 40 yr to establish quasi-steady-state conditions, which were used as initial conditions for the static and warming simulations. Static simulations representing current conditions were run for 10 yr, warming models were run for 85 yr, all at 1-d timesteps. GW temperatures were extracted from the depth of interest over the last year of each simulation and compared to daily stream temperature records from 2014, collected as described in Snyder et al. (2015). The stream water thermal mixing model presented in Kobayashi (1985) was rearranged to predict the cooling capacity (for summer surface-water thermal maxima) of conservative advective mixing of GW seepage (hypothesized 10 and 25% of total channel flow) and stream water to explore the capacity of advective streambed heat exchange with cool channel water for the warmest observed surface water in 2014 and predicted for 2099. This approach assumes GW seepage temperature is not strongly affected by stream channel dynamics.

3. Results

Our numerical models showed that GW seepage will likely be strongly sensitive to annual and decadal air temperature dynamics in this mountainous watershed.

3.1. Stream temperature and channel incision

Channel incision derived from lidar was similar along the upper and lower trout stream sections, averaging 1.4 m depth, and was used to estimate alluvial aquifer unsaturated zone thickness. Rov-

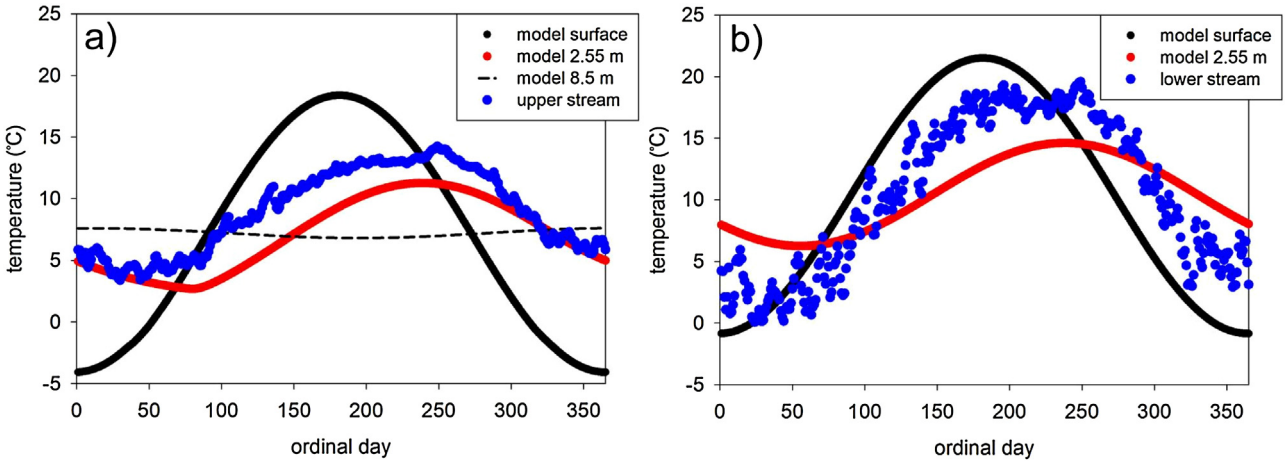

Fig. 4. Model and measured temperature time series from the (a) upper, and (b) lower stream sections. Stream water temperature (2014, blue markers) at the upper site shows less short-term variance and more closely resembles the simulated groundwater temperature (phase shift, max/min), compared to the lower site, indicating strong groundwater influence from the shallow aquifer depth measured with HVSR. A discrete deeper trough of alluvial material was identified near the borehole along the upper stream section, groundwater from this average bedrock contact of 8.5 m was predicted to show little annual variance (dashed line, Panel a). (For interpretation of the references to colour in this figure legend, the reader is referred to the web version of this article.)

ing infrared surveys generally did not indicate deeper GW discharge based on surface temperature (data not shown), except for a few discrete points along the canyon wall in the steep waterfall region; this assessment is consistent with the conceptual model of Nelms and Moberg (2010) that predicted isolated discharge from fractured bedrock at strong slope breaks.

The streambed thermal data showed the strongest diurnal variation from approximately 12/03-12/11/2015, so this subset of data was analyzed with the VFLUX2 program (Briggs et al., 2017a). Thermal diffusivity measurements from the two streambed locations were similar (geometric mean over the period of 0.054 and 0.056 m^2d^{-1}) indicating that even modest streambed diurnal signals (amplitude approximately 0.4 °C) are useful for evaluating thermal diffusivity in situ using new analytical methods (e.g Luce et al., 2013). The average value of 0.055 m^2d^{-1} was converted to the solid-grain thermal conductivity SUTRA model parameter by assuming a specific heat of granite/basalt of 900 $Jkg^{-1}C^{-1}$ (Waples and Waples, 2004), alluvium porosity of 0.4, and weighted arithmetic averaging with the water fraction to determine bulk matrix heat capacity (Table 2). In accordance with the SUTRA model (Voss and Provost, 2002), weighted arithmetic averaging was also assumed for matrix thermal conductivity, yielding a solid alluvial grain value of 2.9 $Js^{-1}m^{-1}C^{-1}$. When recombined in the SUTRA model, the measured value of effective saturated aquifer thermal diffusivity of 0.055 m^2d^{-1} is attained.

One complete year of daily stream temperature records was collected in 2014 for both the main upper and lower stream sections (*US* and *LS*, Fig. 2c and d), and these data were used specifically to compare the numerical aquifer models. The upper stream section water temperature showed visibly less short-term thermal variability in 2014 than the lower section (Fig. 4), indicating a strong thermal buffering GW influence, which corresponds with the findings of Snyder et al. (2015). Further, the minimum 2014 winter stream temperature at the upper site is actually 3.3 °C *warmer* than the lower site (3.39 versus 0.08 °C).

Expanded air/water temperature time series was compared for 3.2 yr at the upper reach and 2.0 yr at the lower reach based on available stream temperature records; for this analysis the main stream sampling points were augmented by nearby stream locations (*US*-2, *LS*-2, Fig. 2c and d) to explore spatial and temporal annual signal characteristics in stream water. Non-stationary sinusoids extracted from the raw temperature data (e.g. Fig. 5a and b) reveal spatially complex relationships between water and air (Fig. 6). The phase of the mixed stream channel annual signal was found to lag the local air signal by approximately 18 d, yet a location just 600 m downstream, still within the upper trout reach, showed a shorter lag of approximately 8 d (Fig. 6a). The main site near the terminus of the lower trout reach had a lag of 14 d that increased over the 2-yr period toward 17 d, similar to the upper main site; a paired site 750 m upstream also showed a positive phase lag trend, from 10.5 to 12 d. The stream "damping factor", or ratio of annual signal amplitude in stream water to surface air (e.g. Kurylyk et al., 2015), was lowest for the main upper stream section *US* site, ranging from 0.41-0.48 (Fig. 6b). The nearby paired site showed a stronger annual signal in stream water, with a damping of approximately 0.66, corresponding with the reduced phase lag discussed above. The downstream trout reach showed even less damping, with ratios ranging from 0.75-0.82, with greater attenuation of the annual signal at the lower main site.

3.2. Geophysical seismic measurements

An example HVSR curve from the top of WOC at a station collocated with borehole W-876 showing a clear seismic resonance peak is presented in Fig. 2d. Using an active seismic technique, an empirically-derived V_S of 346 (stdev 9) ms^{-1} was determined for the unconsolidated sediments adjacent to the existing GW well; the mean of the lower active V_s (346 ms^{-1}) measurements is identical (Briggs et al., 2017b). This result suggests the HVSR method is appropriate to apply throughout the watershed stream corridor using a common V_s, even with a change in parent bedrock (basaltic to granitic), greatly simplifying analysis. HVSR-interpreted sediment thickness from points in the vicinity of the riparian borehole W-876 (reported depth 7.62 m) range from 7.65 to 8.14 m; when the uncertainty of V_s derived from active seismic methods is considered (+/−9 ms^{-1}), two of the three measurements are statistically identical to the reported borehole depth (Table 3). Each HVSR curve was qualitatively assigned a quality score ranging from 1 to 3, where a score of 1 indicates a sharp, clearly resolved resonance peak; 2 indicates a usable, but less-defined peak; and a score of 3 indicates an HVSR curve with characteristics less-suitable for interpretation, but are included here for comparison to other nearby measurements. Two of the 24 HVSR stream transect measurements showed such poor ground coupling that they were excluded from further analysis. Instruments coupled directly to bedrock displayed no defined peak, as expected, but coupling to large boulders sus-

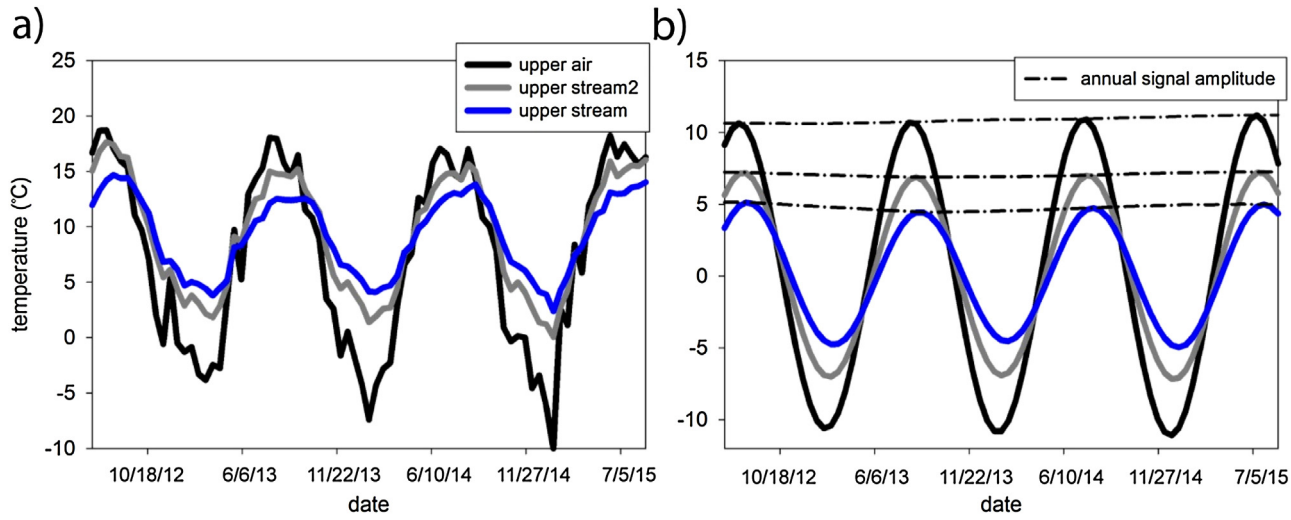

Fig. 5. (Panel a) shows paired raw streamside air and water column temperature from the upper brook trout stream sections for approximately 3 years. The dynamic harmonic regression signal extraction technique was used to extract the fundamental non-stationary sinusoids from each time series (Panel b), allowing a temporal comparison of signal phase lag and amplitude between air and water.

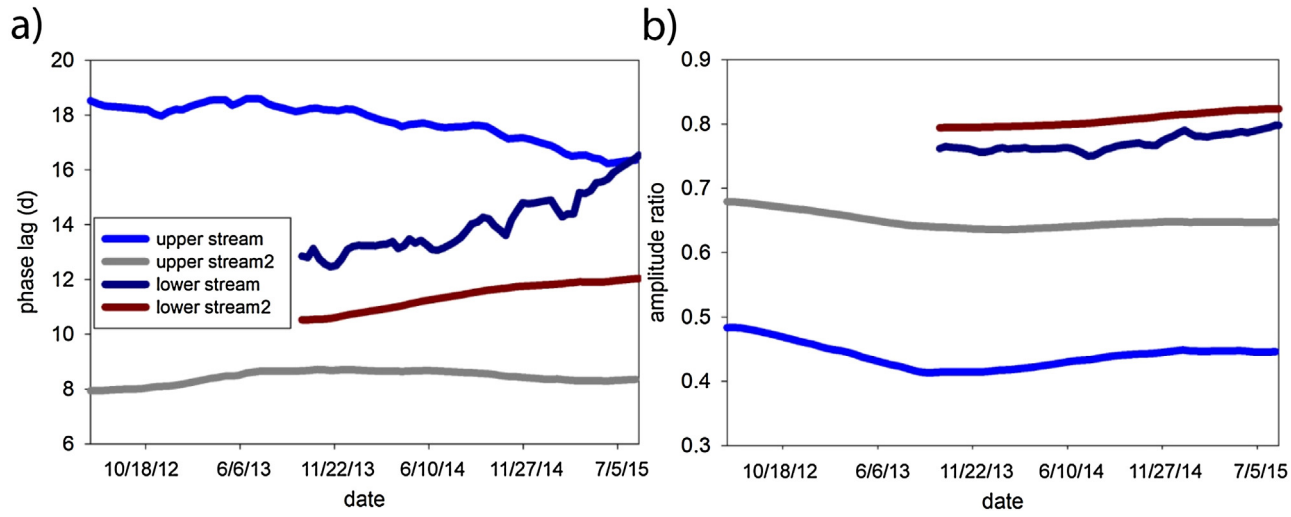

Fig. 6. These time series show the time-variable (a) phase lag, and (b) amplitude ratio (stream damping factor) between the near-stream air and mixed stream water annual temperature signals.

pended in alluvium did yield HVSR resonance peaks, and therefore bedrock outcrop could be distinguished from detached rock.

Neglecting the riparian area around borehole W-876, where HVSR measurements indicated a mean depth of 8.5 m, near-stream HVSR measurements along the upper and lower sections were similar, and show a mean of 2.6 m (Fig. 2c and d, Table 3). GW temperature from the SUTRA models from this depth is primarily used for comparison to observed (2014) stream water records in the context of thermal and climate refugia.

3.3. Vertical aquifer model results

Under the current climate, modeled GW temperature at the 2.6 m depth is predicted to lag ground surface temperature (annual signal) by 59 and 57 d at the upper and lower stream sections, respectively (Fig. 4) (Briggs et al., 2017c). The aquifer damping factor (ratio of annual signal amplitude at depth to surface) is approximately 0.4 for both simulations at 2.6 m; the damping factor for 8.5 m, or the average depth to rock in the borehole riparian zone, is an order of magnitude stronger at 0.04, as GW temperature converges on the annual surface mean (dashed line, Fig. 4a). The phase lag for GW traveling along the average bedrock contact depth within the thicker riparian aquifer zone around the borehole is much longer at 184 d; however, as the annual signal is essentially filtered out by this depth this offset would have minimal importance to the cooling capacity of deeper-derived GW seepage.

Using the method described in Appendix A, the stream water *MWAT* was predicted to be 19.1 and 24.1 °C for the upper and lower current trout habitat sections, respectively. In addition to being at a higher elevation, this prediction factors into the current expected GW influence as evaluated by Snyder et al. (2015). The lower stream section 1D SUTRA aquifer model was run for 85 future years, including a predicted 5 °C mean (linear) air temperature rise over that time. Assuming similar timing of a maximum stream temperature event as was observed on 08/27/2014, the 2.6-m aquifer temperature is predicted to be approximately 19.4 °C at that time in year 2099, reducing cooling capacity in comparison to the current modeled GW temperature at that time in year of 14.5 °C (ΔT approximately 5 °C). These vertical aquifer models indicate shallow

Table 3
The resonance frequencies (f_r) evaluated with the HVSR method, which are converted to a depth to bedrock measurement using the alluvium shear wave velocity (V_s = 346+/−9 ms^{-1}) as evaluated with active seismic methods. Sequential measurements listed in bold were collected at approximately the same land surface location, and the transect measurements are labeled alpha-numerically from high to low elevation as T1...T8, followed by R, M, L, indicating lateral location-downstream right, middle, and left.

location	f_r (Hz)	f_r Q-rating	mean depth (m)	lower bound (m)	upper bound (m)
borehole	**11.31**	**1**	**7.7**	**7.9**	**7.5**
borehole	**11.19**	**1**	**7.7**	**7.9**	**7.5**
borehole	**10.63**	**1**	**8.1**	**8.4**	**7.9**
borehole area	11.94	1	7.2	7.4	7.1
borehole area	10.75	1	8.1	8.3	7.8
borehole area	10.69	1	8.1	8.3	7.9
borehole area	8.88	1	9.7	10.0	9.5
borehole area	8.81	1	9.8	10.1	9.6
basin outlet	14.38	1	6.0	6.2	5.9
basin outlet	13.38	1	6.5	6.6	6.3
T1 R	40.75	1	2.1	2.2	2.1
T1 M	31.13	3	2.8	2.9	2.7
T1 L	35.81	1	2.4	2.5	2.4
T2 M	24.44	1	3.5	3.6	3.5
T2 L	38.25	1	2.3	2.3	2.2
T3 R	42.25	1	2.1	2.1	2.0
T3 M	43.56	1	2.0	2.0	1.9
T4 R	23.69	1	3.7	3.8	3.6
T4 M	57.13	3	1.5	1.6	1.5
T4 L	25.81	3	3.4	3.4	3.3
T5L	**58.69**	**3**	**1.5**	**1.5**	**1.4**
T5M	**63.94**	**1**	**1.4**	**1.4**	**1.3**
T5 R	**50.44**	**1**	**1.7**	**1.8**	**1.7**
T6 L	28.88	1	3.0	3.1	2.9
T6 M	57.88	1	1.5	1.5	1.5
T6 R	23.25	3	3.7	3.8	3.6
T7 L	13.00	1	6.7	6.8	6.5
T7 M	56.19	1	1.5	1.6	1.5
T7 R	53.44	1	1.6	1.7	1.6
T8L	**10.56**	**1**	**8.2**	**8.4**	**8.0**
T8M	**9.50**	**3**	**9.1**	**9.3**	**8.9**
T8 R	31.44	1	2.8	2.8	2.7

GW temperature will closely track surface climate warming in SNP mountain watersheds.

4. Discussion

The two main trout stream reach sites showed annual temperature signals that lagged local air signals by approximately 2.5 weeks. This markedly contrasts previously published stream temperature data (e.g. Mohseni and Stefan, 1999), which indicate long-term temperature signals are typically in-phase between stream water and local air, or show lags on the order of a few days (Caissie et al., 2005). Hyporheic exchange has been shown to reduce short-term stream channel water temperature fluctuations (e.g. diurnal) (Johnson, 2004), but not to lag long-period annual thermal signals. The unique stream water temperature lags observed here indicate strong stream channel heat exchange with shallow GW, which is predicted to lag air temperature changes.

4.1. Sensitivity of current groundwater-driven climate refugia to air temperature

Precipitation on steep terrain is expected to induce relatively deep infiltration in some settings (Jasechko et al., 2016), resulting in longer residence times and highly attenuated surface thermal signals. However, in the older geologic setting of the Appalachian highlands where bedrock is shallow and of low permeability, aquifer residence time may be short (e.g., <3 years, in Plummer et al., 2001), shallow GW temperature will be dynamic over yearly timescales. In similar systems dominated by shallow horizontal flow along a laterally contiguous bedrock contact, the effect of aquifer depth will dominate GW temperature, and actual water residence time will be of minimal importance to seepage zone temperature. This reduces the complexity involved in predicting the future of climate refugia zones in similar mountain stream systems that are sustained by shallow GW.

Although annual air temperature dynamics are often assumed to dominate stream temperature throughout the year (e.g. Mohseni and Stefan, 1999), as discussed by Kurylyk et al. (2016), forested streams may be strongly controlled by the thermal influence of GW advection and conduction, which is supported by our observations and analyses. The observed stream water temperature phase lag at the main upper trout section site (18 d, Fig. 6a) is less than the model simulation at 2.6 m depth (60 d), but quite similar to the shallow aquifer modeled winter minimum temperature (Fig. 4a) and annual signal damping factor (approximately 0.4). This result suggests strong GW thermal influence from the thin alluvial aquifer inferred through HVSR measurement (Fig. 2c). The phase lag is relatively consistent over annual cycles, indicating the upper stream section is dominated by shallow base flow throughout the year, which has also been indicated through hydrograph separation for similar streams in the SNP (Nelms and Moberg, 2010). Seepage from deeper GW flowpaths (e.g. >approximately 8 m depth here) would be expected to buffer stream water temperature signals expressed by the stream damping factor, but not induce a prominent phase lag as GW temperature at depth shows little annual signal (Figs. 1, 4 a).

As has been shown with shorter-term paired air/water sensitivity metrics (e.g. Snyder et al., 2015), the influence of GW along this stream network is patchy, with even the long-period annual signals changing strongly relative to air over hundreds of meters of channel distance in the upper section. The buffering effect of GW seepage on seasonal stream water temperature dynamics, expressed by the annual stream damping factor, is greatly reduced 600 m downstream of the main upper section site. Brook trout spawn in fall and incubate eggs within gravel redds (nests) over winter months, so localized GW seepage in SNP likely protects trout eggs

from anchor ice while accelerating egg development (Curry et al., 1995). Upwelling zones also provide warm refugia during winter months (Cunjak and Power, 1986) and cold refugia during summer months for juvenile and adult fishes (Petty et al., 2012). Coldest winter stream temperature observed in 2014 were actually more extreme at the lower-elevation trout reach compared to the higher-elevation trout section (0.08 versus 3.39 °C, Fig. 4); this relative stream water warming induced by even shallow groundwater discharge is likely influential to winter brook trout egg development (French et al., 2016). It is interesting to note that at the lower site observed strong annual phase lag (increasing over time to 17d) corresponds with only a small decrease in the stream damping factor. Future work using total stream heat budget models should consider investigating the complicated interplay between aquifer depth-specific GW seepage and channel water temperature dynamics.

The warmest 2014 water temperatures occurred on 09/05/2014 at the upper (14.3 °C) and lower (19.6 °C) sections, well within brook trout thermal tolerance limits, and falling somewhat later than would be predicted by the general annual temperature dynamics. Due to the annual phase lag predicted at the 2.6 m bedrock contact, GW from this depth shows a temperature maxima only ~11 d prior; in contrast, simulated GW at the 8.5 m depth (borehole riparian area) shows a thermal maxima on the last day of the year. These results illustrate that although the lag between average SW and GW temperature dynamics should increase GW cooling potential, warm air weather patterns later in the summer may occur closer to shallow GW thermal maxima, reducing the potential (ΔT) for advective and conductive cooling at that time.

Assuming conservative thermal mixing of stream and GW (Kobayashi, 1985), and no modification of GW temperature along the subsurface flow path to the stream, a mixture of 10% GW by volume would change the upper and lower trout section maximum 2014 stream water temperatures by −0.3 and −0.5 °C, respectively; and a large 25% GW infusion would decrease stream temperature by −0.8 and −1.4 °C, respectively. For comparison, if GW from the borehole riparian zone at 8.5 m entered the upper stream via pipe-flow (GW temperature not affected by downward conduction before discharge), a 25% mixture would cool channel water by −2.0 °C. This result clearly shows how shallow GW, restricted by low permeability bedrock, has reduced potential to generate thermal and climate refugia for cold water species compared to deeper GW that approximates mean annual temperature.

Although the HVSR measurements were well distributed longitudinally along the upper and lower trout habitat stream sections, measurement transects were confined to the near-stream area. In many locations exposed bedrock was visible along the lateral valley walls, so it was assumed alluvial sediments along the stream corridor would generally represent the deepest sections of the unconsolidated aquifer. Further, GW flowing laterally toward the stream would need to filter through near-stream aquifer material, and, at typical GW flow rates (<0.5 md^{-1}, Alley et al., 1999), would assume the thermal signature of those sediments that are dominated by surface conduction. In this manner riparian sediments likely act as a thermal modifier of larger-scale hillslope GW discharge to streams when vertical infiltration is impaired by a shallow bedrock surface, and are therefore critical to evaluate for thickness in the context of thermal climate refugia. It should be noted that upwelling GW may experience further heat exchange (warming in summer) with channel water as it approaches the sediment-water interface, a concept currently not well accounted for in ecological habitat modeling (Kurylyk et al., 2016). However, as this conductive exchange effectively transfers heat from the channel water, the net cooling effect on stream temperature may be similar to a scenario where discrete, strong seepage enters the stream at local average GW temperature (e.g. Hare et al., 2015); further research is needed to better define the reach-scale "streambed radiator" effect of conductive heat exchange over focused and diffuse seepage zones, which will vary by alluvial aquifer rock/sediment type, due to varied matrix thermal diffusivities.

Two areas in WOC stand out as having alluvial sediment thicknesses much greater than the majority of near-stream HVSR measurements. At the outlet of the watershed a broad outwash fan exists, consisting of materials mobilized at the highest flows and mass wasting. Approximately 60 m lateral to the most braided channel, a terrace of coarse material stands several meters above the near-stream sediments. HVSR measurements collected at similar locations on this terrace indicated depths to rock of 8.2 and 9.1 m; HVSR collected off the terrace closer to the stream indicated a depth of 2.8 m. Clearly infiltration into the terrace deposit may adopt a thermal signature close to the annual ground surface mean, but as this water travels laterally (60 m+) toward the stream it would pass through the thin, thermally dynamic near-stream sediments. Along the upper section in an area within approximately 40 m of the borehole (reported depth 7.62 m), HVSR measurements indicated an average depth to rock of 8.5 m. This saddle in the bedrock is water bearing, as was noted by the original drilling report description of the area as a "wetland" (DeKay, 1972), and there was visual confirmation of apparent surface springs during a precipitation event during HVSR data collection. The thermal signature of this water will be more complicated, and likely represents an integration of GW flowpath depths that are forced to the surface in this area, similar to scenarios depicted by Kurylyk et al. (2015). This thicker near-stream alluvial aquifer, which would be expected to be more thermally-resilient to climate dynamics, seems to be an exception in this watershed, and indeed in SNP at large (Lynch, 1987).

4.2. The viability of future climate refugia for native brook trout

The upper reach, approximately 600 m higher in elevation, will likely maintain a *MWAT* of <20 °C over this time. This is fortunate, as the steep waterfall region through the central watershed (Fig. 2a and b) would likely inhibit natural trout recolonization of the upper-reach should expatriation occur due to warm SW events. The current lower preferential stream habitat at WOC will likely exceed the general 23.3 °C *MWAT* limit for brook trout survival by 2099, reaching an estimated weekly mean of 24.1 °C using the prediction method described in Appendix A. Therefore the viability of the lower stream section to support brook trout throughout the year may be strongly influenced by possible GW seepage. At the lower site, a large seepage zone contributing 25% of channel water would only lower mixed water temperature on the warmest day to 23.5 °C, and exceed the *MWAT* for over 7 contiguous d. This result indicates larger-scale climate refugia may be compromised in the lower watershed by year 2099, and brook trout may be restricted to the upper section, or forced to find refuge in isolated thermal refugia impacted by unmixed or deeper GW at lower elevations. As mentioned above, the waterfall region in WOC presents a physical barrier to the upstream migration of fish seeking to escape warming SW.

5. Conclusions

Here, we have demonstrated that passive seismic HVSR can be an effective method for measuring depth to bedrock underlying stream networks. Vertical numerical simulations informed by sediment thickness data can be used to predict shallow near-stream aquifer thermal sensitivity to local air dynamics, and are improved with in-situ measurements of aquifer thermal diffusivity, which can now be done using natural diurnal signals (e.g. Irvine et al., 2015). Heat tracing methods applied to stream water, such as fiber-optic distributed temperature sensing or thermal infrared

imagery, can yield important geospatial information regarding GW discharge points, but less understanding of upgradient GW flowpath dynamics. We show that multiple-year paired air and stream water temperature data can indicate whether GW flowpaths are near surface, and therefore inherently more sensitive to a dynamic climate. Stream water annual sinusoids will show greater damping from the driving atmospheric signal when influenced by GW seepage; when the mixed stream water signal shows a phase-shift as well, seepage is likely sourced by shallow GW flowpaths. Here, non-stationary annual temperature sinusoids extracted from paired local air and stream water sites indicate long-term (here 3+ years) spatiotemporal patterns of seepage influence. Strong GW seepage originating from the upper approximately 2.6 m of aquifer material may explain the unique large lags observed between annual air and stream water temperature (e.g. 18 d) that, along with the stream damping factor, were variable along the network. Coupled stream water and adjacent aquifer temperature predictions indicate lower-elevation streams in SNP may not support brook trout by 2099, even with a strong (e.g. 25% total flow) local GW seepage influence, because the shallow alluvial aquifer will closely track surface warm summer temperatures. Overall, measured spatial variability in depth to bedrock can be used to improve statistical models for predicting future stream temperature at ecologically relevant spatial scales across the mountain watersheds that currently support native brook trout.

Acknowledgments

The authors acknowledge support from the U.S. Geological Survey (USGS) Chesapeake Bay Priority Ecosystems Science and Fisheries Program, USGS Natural Resource Preservation Program, USGS Office of Groundwater, USGS National Research Program, USGS Groundwater Resources Program, and the USGS Toxic Substances Hydrology Program. We also thank the National Park Service for site access and general support. The data described in this manuscript are available from Data.gov as specified in the reference list. Any use of trade, firm, or product names is for descriptive purposes only and does not imply endorsement by the U.S. Government.

Appendix A.

We simulated future summer daily air and water temperature regimes at the upper and lower Whiteoak Canyon watershed sites under a 5 °C increase in mean annual air temperature climate scenario. This temperature increase roughly corresponds to the median increase predicted for eastern North America by alternative global circulation models and emission scenarios for the 30-year period ending in 2099, relative to a baseline period defined as 1961–1990 (Horton et al., 2014). We examined historical daily air temperature records from 1944 to 2014 from a National Park Service weather station located on the western boundary of the park in Luray, Virginia, and computed the mean annual and mean summer water temperature for the 1961–1990 baseline period (Appendix Fig. A1). We found that the 2014 study year, a year where we had collected complete daily air and water temperatures at both study sites, closely approximated baseline average annual and summer air temperature. Therefore, we used the 2014 study year to represent regional baseline climate. We simulated the 2099 air temperature regime by increasing the mean annual air temperature observed at each site by 5 °C, then downscaling to daily time steps by assuming daily air temperature variation patterns for the future climate would correspond exactly as they did in 2014 (e.g. Snyder et al., 2015, Appendix Fig. A2(A)).

Table A1
Results of site-specific regression modeling to predict daily water temperatures from daily air temperature data at two the Whiteoak Canyon watershed sites in Shenandoah National Park. For each of the two predictor variables we show the model coefficients as well as the partial R^2 value (in parentheses).

Site	Model Coefficients			Model Statistics	
	Y-intercept	Air_0	Air_{50}	Adj. R^2	RMSE
Upper	5.469	0.064 (0.159)	0.354 (0.817)	0.976	0.500
Lower	2.302	0.371 (0.531)	0.370 (0.441)	0.972	1.020

Hourly air and water temperature data for the 2014 study year were collected with Onset ProV2 temperature loggers (Onset Computer Corp., Cape Cod, USA) at each site and summarized as daily mean temperature. We used site-specific air-water regression models generated from daily data collected in 2014 to predict future daily water temperature regimes at both sites. From the observed air temperature data, we derived two air temperature variables; the daily mean air temperature observed on day_i (Air_0), and the 50-day running average leading up to day_i (Air_{50}) as predictor variables in our regression models to predict water temperature on day_i. We found from previous analyses that the smoothed Air_{50} variable correlated with seasonal changes in GW temperature, and the Air_0 correlated with water temperature on day_i for sites dominated by runoff. Together, these two air temperature variables were effective predictors of water temperatures at 78 individual stream reaches in Shenandoah National Park that varied in terms of groundwater contribution (Snyder et al., 2015). For the two Whiteoak Canyon sites, the two-variable models accounted for over 97% of variation in daily water temperature observed in 2014 (adjusted $R^2 > 0.97$) at both sites, and the root mean square error (RSME) was 0.500 °C for the upper site and 1.02 °C for the lower site. We used the partial R^2 for the two variables to infer relative influence of runoff and groundwater. The upper site had partial R^2 values of 0.16 and 0.82 for the Air_0 and Air_{50} terms, respectively, indicating surface flow was composed largely of shallow GW; whereas partial R^2 values for the lower site were 0.44 and 0.53, respectively, indicating approximately equal contributions from runoff and shallow GW (Table A1).

Though effective in predicting current water temperature, these regression models cannot be used directly to predict future stream temperatures because they do not explicitly account for the potential of GW temperatures to increase with long-term (e.g., annual or decadal) changes in climate (Kurylyk et al., 2013). To account for long-term changes in GW temperature, we made use of the observation that in reaches where flow is dominated by GW, the y-intercept of air-water temperature regressions approximates regional GW temperature, whereas in runoff-dominated sites the y-intercept approximates zero (Caissie, 2006). Snyder et al. (2015) found that the y-intercept term of these models was linearly related to Air_{50} (the partial R^2 for the air temperature term correlated with GW in this case). Thus, under future climate, the y-intercept should be adjusted in proportion to GW contribution (inferred from the partial R^2 value for the Air_{50} term). Assuming that the shallow GW sources typical in Shenandoah National Park (Plummer et al., 2001) respond to changes in long-term air temperature in a 1:1 manner, then a 5 °C increase in mean annual air temperature would result in a 5 °C increase in the y-intercept term at sites completely dominated by GW (partial R^2 $Air_{50} = 1$); whereas the y-intercept would not change at sites with no GW contribution (partial R^2 $Air_{50} = 0$). Snyder et al. (2015) found that estimates of GW temperature showed an approximately 1:1 relationship with mean annual air temperature of the preceding year suggesting that shallow GW in the park is highly sensitive to annual variation in air temperature and that our assumption regarding GW thermal sensitivity is reasonable for long-term predictions. In addition, from predicted

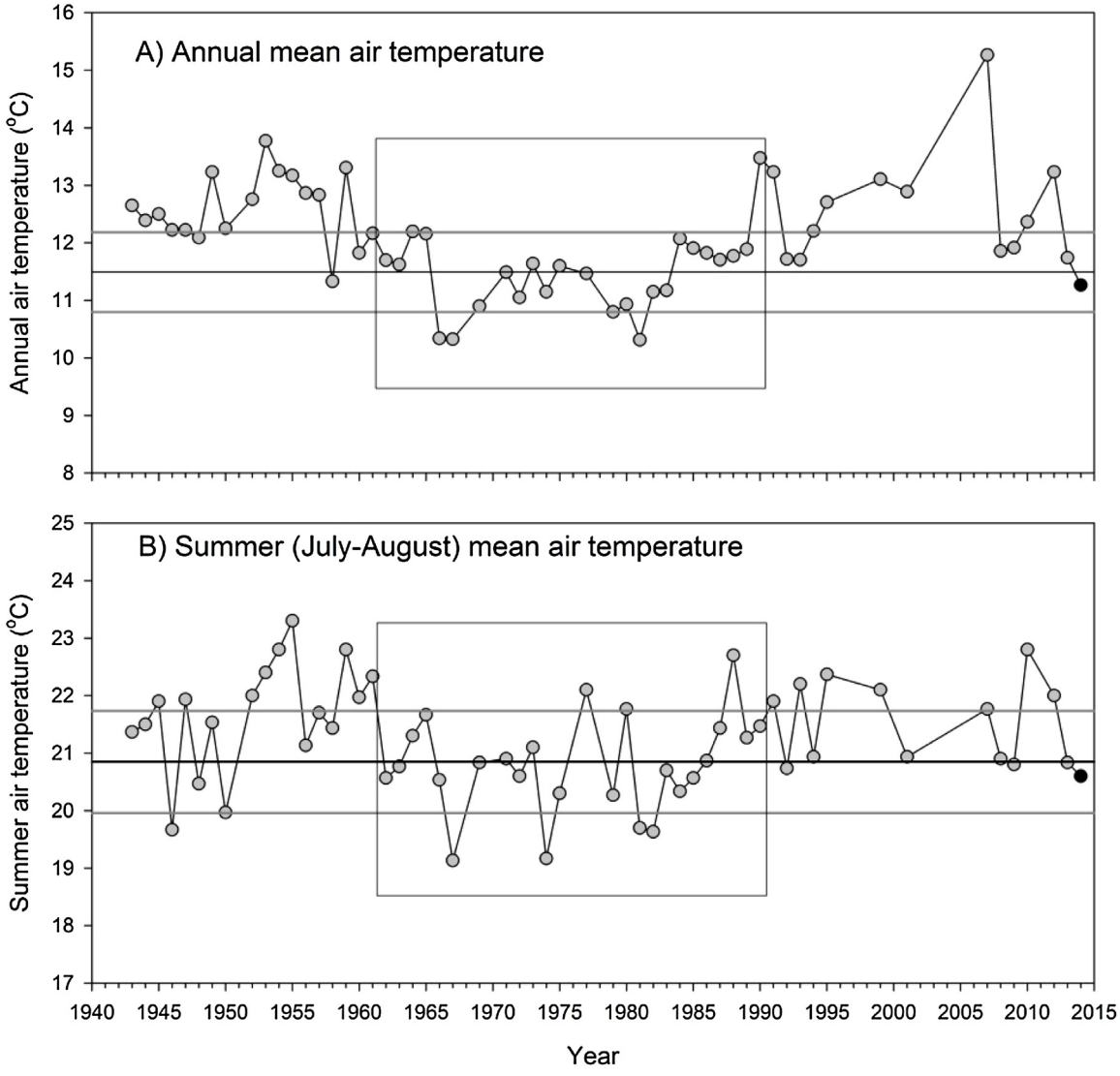

Fig. A1. Annual (A) and summer (B) air temperature records for the years 1944–2015 from the Shenandoah National Park weather station located at Luray, Virginia. The black boxes contain records from 1961 to 1990, representing the baseline period for predicting future climates, and the horizontal lines represent the baseline mean (black) +/−1 S.D. (gray) for the annual and summer periods. The 2014 study year (black circle) was used to represent baseline daily thermal regimes in our simulations.

summer water temperature regimes, we were able to estimate brook trout thermal habitat suitability using a threshold of 23.3 °C mean weekly average temperature (MWAT), wherein MWAT values that exceed the threshold are deemed thermally unsuitable (Wehrly et al., 2007). MWAT is computed as the maximum of the running 7-day averages of daily mean water temperatures. Current (2014) and simulated future (2099) water temperature regimes (running 7-day averages) for the summer season generated from our air-water regression models are shown in Appendix Fig. A2(B).

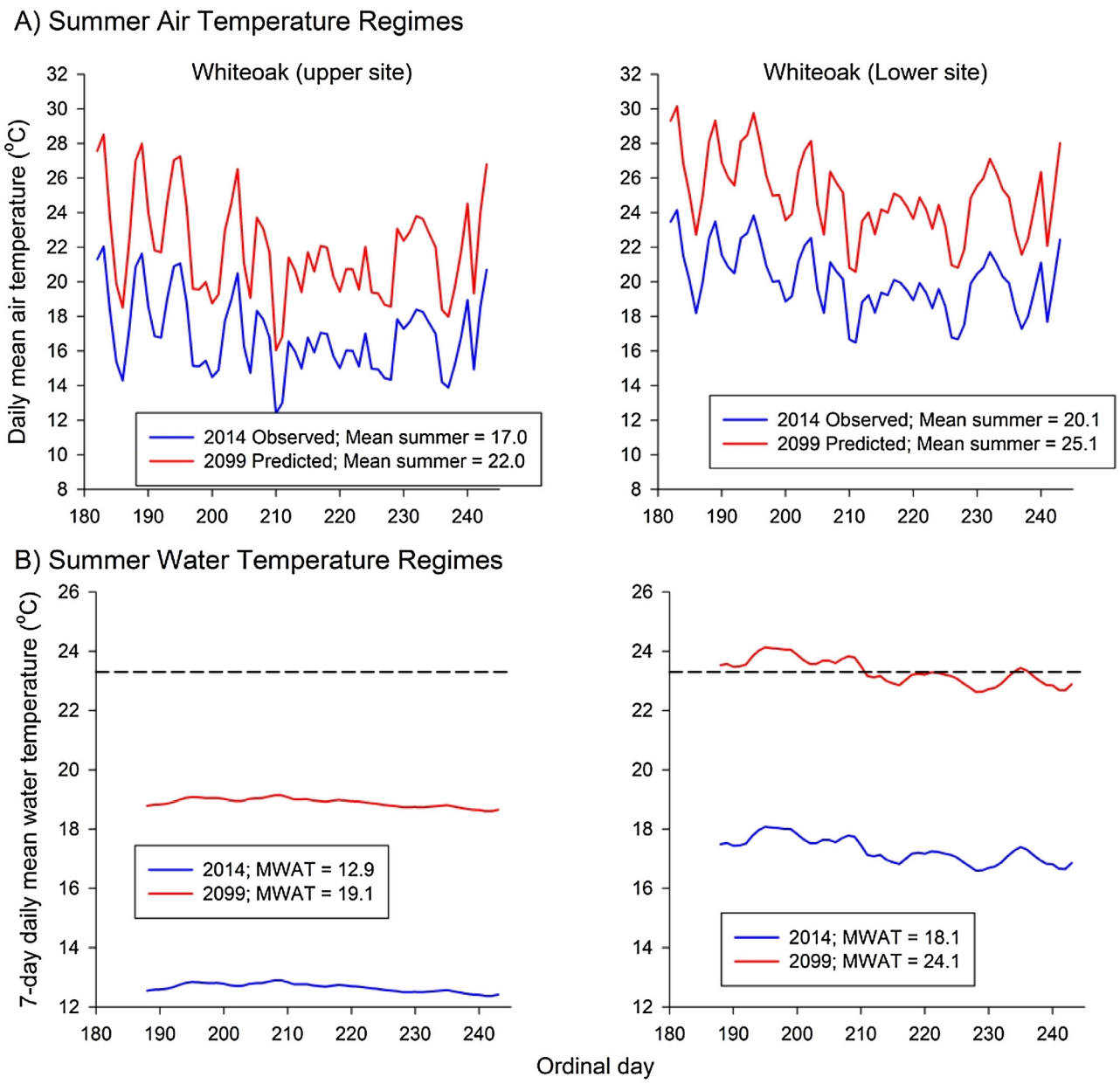

Fig. A2. Summer air (A) and water (B) temperature regimes for the upper (left panels) and lower (right panels) sites in Whiteoak Canyon watershed under current (2014) and simulated future (2099) climates (see text for details regarding simulation methods). Air temperature regimes show daily mean air temperatures and water temperature regimes show the 7-day running average daily mean air temperatures used to compute maximum weekly average temperature (*MWAT*, dashed line).

References

Alley, W.M., Reilly, T.E., Franke, O.L., 1999. Sustainability of ground-water Resources. U.S. Geol. Surv. Circ. 1186, 79.

Arrigoni, A.S., Poole, G.C., Mertes, L.A.K., Daniel, S.J.O., Woessner, W.W., Thomas, S.A., 2008. Buffered, lagged, or cooled? Disentangling hyporheic influences on temperature cycles in stream channels. Water Resour. Res. 44, 1–13.

Bergstrom, A., McGlynn, B., Mallard, J., Covino, T., 2016. Watershed structural influences on the distributions of stream network water and solute travel times under baseflow conditions. Hydrol. Process. 30, 2671–2685.

Binley, A., Hubbard, S.S., Huisman, J.A., Revil, A., Robinso, D.A., Singha, K., Slater, L.D., 2015. The emergence of hydrogeophysics for improved understanding of subsurface processes over multiple scales. Water Resour. Res. 51, 1–30.

Bonnefoy-Claudet, S., Cotton, F., Bard, P.Y., 2006. The nature of seismic noise wavefield and its implications for site effects studies. Earth Sci. Rev. 23.

Briggs, M.A., Voytek, E.B., Day-Lewis, F.D., Rosenberry, D.O., Lane, J.W., 2013. Understanding water column and streambed thermal refugia for endangered mussels in the delaware river. Environ. Sci. Technol. 47, 11423–11431.

Briggs, M.A., Walvoord, M.A., Mckenzie, J.M., Voss, C.I., Day-Lewis, F.D., Lane, J.W., 2014. New permafrost is forming around shrinking Arctic lakes, but will it last? Geophys. Res. Lett., 1–8.

Briggs, M.A., Lane, J.W., Snyder, C.D., White, E.A., Johnson, Z.C., Nelms, D.L., Hitt, N.P., 2017a. Temperature Data for Study of Shallow Mountain Bedrock Limits Seepage-Based Headwater Climate Refugia. U.S. Geological Survey Data Release, Shenandoah National Park, Virginia, http://dx.doi.org/10.5066/F7TD9VFS.

Briggs, M.A., Lane, J.W., Snyder, C.D., White, E.A., Johnson, Z.C., Nelms, D.L., Hitt, N.P., 2017b. Seismic Data for Study of Shallow Mountain Bedrock Limits Seepage-Based Headwater Climate Refugia. U.S. Geological Survey Data Release, Shenandoah National Park, Virginia, http://dx.doi.org/10.5066/F7JW8C04.

Briggs, M.A., Lane, J.W., Snyder, C.D., White, E.A., Johnson, Z.C., Nelms, D.L., Hitt, N.P., 2017c. Modeled Temperature Data Developed for Study of Shallow Mountain Bedrock Limits Seepage-Based Headwater Climate Refugia. U.S. Geological Survey Data Release, Shenandoah National Park, Virginia, http://dx.doi.org/10.5066/F7F47M8Q.

Busenberg, E., Plummer, L.N., Coplen, T.B., Doughten, M.W., Widman, P.K., Casile, G.C., Wayland, J.E., Nelms, D., 2014. Shenandoah national park a 19-Year record of chemical and isotopic composition of water from springs of the Shenandoah National Park, Virginia, 1995–2014. U.S. Geol. Surv. Data Ser. 893, 11.

Caissie, D., Satish, M.G., El-Jabi, N., 2005. Predicting river water temperatures using the equilibrium temperature concept with application on Miramichi River catchments (New Brunswick, Canada). Hydrol. Process. 19, 2137–2159.
Caissie, D., Kurylyk, B.L., St-Hilaire, A., El-Jabi, N., MacQuarrie, K.T.B., 2014. Streambed temperature dynamics and corresponding heat fluxes in small streams experiencing seasonal ice cover. J. Hydrol. 519, 1441–1452.
Caissie, D., 2006. The thermal regime of rivers: a review. Freshw. Biol. 51, 1389–1406.
Campbell, B.G., Landmeyer, J.E., 2014. Groundwater availability in the Crouch Branch and McQueen Branch aquifers, Chesterfield county, South Carolina, 1900–2012. U.S. Geol. Surv. Sci. Investig. Rep. 2014–5050, 68.
Constantz, J., 2008. Heat as a tracer to determine streambed water exchanges. Water Resour. Res. 44, 1–20.
Cunjak, R.A., Power, G., 1986. Seasonal changes in the physiology of brook trout, Salvelinus fontinalis (Mitchill), in a sub-Arctic river system. J. Fish Biol. 29, 279–288.
Curry, R., Noakes, D.L.G., Morgan, G.E., 1995. Groundwater and the incubation and emergence of brook trout (Salvelinus fontinalis). Can. J. Fish. Aquat. Sci. 52, 1741–1749.
DeKay, R.H., 1972. Development of ground-water supplies in Shenandoah National Park, Virginia. Virginia Div. Miner. Resour. Rep. 10, 158.
Delgado, J., López Casado, C., Giner, J., Estévez, A., Cuenca, A., Molina, S., 2000. Microtremors as a geophysical exploration tool: applications and limitations. Pure Appl. Geophys. 157, 1445–1462.
Dugdale, S.J., Bergeron, N.E., St-Hilaire, A., 2015. Spatial distribution of thermal refuges analysed in relation to riverscape hydromorphology using airborne thermal infrared imagery. Remote Sens. Environ. 160, 43–55.
Ebersole, J.L., Liss, W.J., Frissell, C.A., 2003. Cold water patches in warm streams: physicochemical characteristics and the influence of shading. J. Am. Water Resour. Assoc. 59860, 355–368.
Eggleston, J., McCoy, K.J., 2015. Assessing the magnitude and timing of anthropogenic warming of a shallow aquifer: example from Virginia Beach, USA. Hydrogeol. J. 23, 105–120.
Fairchild, G.M., Lane, J.W., Voytek, E.B., Leblanc, D.R., 2013. Bedrock topography of western Cape Cod Massachusetts, based on bedrock altitudes from geologic borings and analysis of ambient seismic noise by the horizontal-to-vertical spectral-ratio method. U.S. Geol. Surv. Sci. Investig. Map 3233, 17.
French, W.E., Vondracek, B., Ferrington, L.C., Finlay, J.C., Dieterman, D.J., 2016. Brown trout (Salmo trutta) growth and condition along a winter thermal gradient in temperate streams. Can. J. Fish. Aquat. Sci. 9, 1–9.
Fry, F.E., Hart, J.S., Walker, K.F., 1946. Lethal temperature relations for a sample of young speckled trout, Salvelinus fontinalis. Univ. Toronto Biol. Ser. 54, 9–35.
Gordon, R.P., Lautz, L.K., Briggs, M.A., McKenzie, J.M., 2012. Automated calculation of vertical pore-water flux from field temperature time series using the VFLUX method and computer program. J. Hydrol. 420–421, 142–158.
Hare, D.K., Briggs, M.A., Rosenberry, D.O., Boutt, D.F., Lane, J.W., 2015. A comparison of thermal infrared to fiber-optic distributed temperature sensing for evaluation of groundwater discharge to surface water. J. Hydrol. 530, 153–166.
Horton, R., Yohe, G., Easterling, W., Kates, R., Ruth, M., Sussman, E., Whelchel, A., Wolfe, D., Lipschultz, F., 2014. Ch. 16: Northeast. Climate Change Impacts in the United States: The Third National Climate Assessment. In: Melillo, J.M., Richmond, T.C., Yohe, G. (Eds.). U.S. Global Change Research Program, pp. 1–24.
Hudy, M., Thieling, T.M., Gillespie, N., Smith, E.P., 2008. Distribution, status, and land use characteristics of subwatersheds within the native range of brook trout in the Eastern United States. North Am. J. Fish. Manage. 28, 1069–1085.
Ibs-von Seht, M., Wohlenberg, J., 1999. Microtremors measurements used to map thickness of soft soil sediments. Bull. Seismol. Soc. Am. 89, 250–259.
Irvine, D.J., Lautz, L.K., Briggs, M.A., Gordon, R.P., Mckenzie, J.M., 2015. Experimental evaluation of the applicability of phase, amplitude, and combined methods to determine water flux and thermal diffusivity from temperature time series using VFLUX 2. J. Hydrol. 531, 728–737.
Irvine, D.J., Cartwright, I., Post, V.E.A., Simmons, C.T., Banks, E.W., 2016. Uncertainties in vertical groundwater fluxes from 1-D steady state heat transport analyses caused by heterogeneity, multidimensional flow, and climate change. Water Resour. Res., 1–20.
Isaak, D.J., Wollrab, S., Horan, D., Chandler, G., 2012. Climate change effects on stream and river temperatures across the northwest U.S. from 1980–2009 and implications for salmonid fishes. Clim. Change 113, 499–524.
Isaak, D.J., Young, M.K., Nagel, D.E., Horan, D.L., Groce, M.C., 2015. The cold-water climate shield: delineating refugia for preserving salmonid fishes through the 21st century. Glob. Chang. Biol. 21, 2540–2553.
Isaak, D.J., Young, M.K., Luce, C.H., Hostetler, S.W., Wenger, S.J., Peterson, E.E., Ver, J.M., Groce, M.C., Horan, D.L., Nagel, D.E., 2016. Slow climate velocities of mountain streams portend their role as refugia for cold-water biodiversity. Proc. Natl. Acad. Sci. U. S. A., 1–6.
Jasechko, S., Kirchner, J.W., Welker, J.M., McDonnell, J.J., 2016. Substantial proportion of global streamflow less than three months old. Nat. Geosci. 9, 7–11.
Jencso, K.G., McGlynn, B.L., Gooseff, M.N., Bencala, K.E., Wondzell, S.M., 2010. Hillslope hydrologic connectivity controls riparian groundwater turnover: implications of catchment structure for riparian buffering and stream water sources. Water Resour. Res. 46, 1–18.
Johnson, S.L., 2004. Factors influencing stream temperatures in small streams: substrate effects and a shading experiment. Can. J. Fish. Aquat. Sci. 61, 913–923.
Kanno, Y., Pregler, K., Hitt, N.P., Letcher, B., Hocking, D., Wofford, J., 2016. Seasonal temperature and precipitation regulate brook trout young-of-the-year abundance and population dynamics. Freshw. Biol. 61, 88–99.
Kelleher, C., Wagener, T., Gooseff, M., McGlynn, B., McGuire, K., Marshall, L., 2012. Investigating controls on the thermal sensitivity of Pennsylvania streams. Hydrol. Process. 26, 771–785.
Kobayashi, D., 1985. Separation of the snowmelt hydrograph by stream temperatures. J. Hydrol. 76, 155–162.
Kurylyk, B.L., Bourque, C.P., MacQuarrie, K.T.B., 2013. Potential surface temperature and shallow groundwater temperature response to climate change: an example from a small forested catchment in east-central New Brunswick (Canada). Hydrol. Earth Syst. Sci. 17, 2701–2716.
Kurylyk, B.L., MacQuarrie, K.T.B., Voss, C.I., 2014. Climate change impacts on the temperature and magnitude of groundwater discharge from shallow, unconfined aquifers. Water Resour. Res. 50, 3253–3274.
Kurylyk, B.L., MacQuarrie, K.T.B., Caissie, D., McKenzie, J.M., 2015. Shallow groundwater thermal sensitivity to climate change and land cover disturbances: derivation of analytical expressions and implications for stream temperature modeling. Hydrol. Earth Syst. Sci. 19, 2469–2489.
Kurylyk, B.L., Moore, R.D., Macquarrie, K.T.B., 2016. Scientific briefing: quantifying streambed heat advection associated with groundwater-surface water interactions. Hydrol. Process. 992, 987–992.
Lane, J.W., White, E.A., Steele, G.V., Cannia, J.C., 2008. Estimation of bedrock depth using the horizontal-to-vertical (H/V) ambient-noise seismic method. In: Application of Geophysics to Engineering and Environmental Problems. Environmental and Engineering Geophysical Society, Philadelphia, p. 13.
Luce, C.H., Tonina, D., Gariglio, F., Applebee, R., 2013. Solutions for the diurnally forced advection-diffusion equation to estimate bulk fluid velocity and diffusivity in streambeds from temperature time series. Water Resour. Res. 49, 488–506.
Lynch, D.D., 1987. Hydrologic conditions and trends in henandoah National Park, Virginia, 1983–84. Water Resour. Investig. Rep., 87–4131.
MacCrimmon, H.R., Campbell, S.C., 1969. World distribution of brook trout, Salaelinus fontinalis. J. Fish. Res. Board Canada 26.
Mathews, K.R., Berg, N.H., 1997. Rainbow trout responses to water temperature and dissolved oxygen stress in two southern California stream pools. J. Fish Biol. 59, 50–67.
McKenzie, J.M., Voss, C.I., 2013. Permafrost thaw in a nested groundwater-flow system. Hydrogeol. J. 21, 299–316.
Mckenzie, J.M., Siegel, D.I., Rosenberry, D.O., Glaser, P.H., Voss, C.I., 2007. Heat transport in the Red Lake Bog, Glacial Lake Agassiz Peatlands. Hydrol. Process. 378, 369–378.
McWhorter, D.B., Sunada, D.K., 1977. Ground- Water Hydrology and Hydraulics. Water Resources Publications, Fort Collins, Colorado.
Meisner, J.D., 1990. Potential loss of thermal habitat for brook trout, due to climatic warming, in two Southern Ontario streams. Trans. Am. Fish. Soc. 119, 282–291.
Mohseni, O., Stefan, H.G., 1999. Stream temperature air temperature relationship: a physical interpretation. J. Hydrol. 218, 128–141.
Mucciarelli, M., Gallipoli, M.R., 2001. A critical review of 10 years of Nakamura technique. Boll. Geof. Teor. Appl. 42, 255–256.
Nakamura, Y., 1989. A method for dynamic characteristics estimations of subsurface using microtremors on the ground surface. Q. Rep. RTRI Japan 30, 25–33.
Nelms, D.L., Moberg, R.M., 2010. Hydrogeology and Groundwater Availability in Clarke County, Virginia. U.S. Geol. Surv. Sci. Investig. Rep. 2010–5112, 119.
O'Reilly, C.M., Sharma, S., Gray, D., Hampton, S., Read, J., Rowley, R., Schneider, P., Lenters, J., McIntyre, P., Kraemer, B., Weyhenmeyer, G., Straile, D., Dong, B., Adrain, R., Allan, M., Anneville, O., Arvola, L., Austin, J., Bailey, J., 2015. Rapid and highly variable warming of lake surface waters around the globe. Geophys. Res. Lett. 42, 10773–10781.
Parolai, S., Bormann, P., Milkert, C., 2002. New relationships between Vs, thickness of sediments, and resonance frequency calculated by the H/V ratio of seismic noise for Cologne area (Germany). Bull. Seismol. Soc. Am. 92, 2521–2527.
Payn, R.A., Gooseff, M.N., McGlynn, B.L., Bencala, K.E., Wondzell, S.M., 2009. Channel water balance and exchange with subsurface flow along a mountain headwater stream in Montana, United States. Water Resour. Res. 45.
Petty, J.T., Hansbarger, J.L., Huntsman, B.M., Mazik, P.M., 2012. Transactions of the American fisheries society brook trout movement in response to temperature, flow, and thermal refugia within a complex appalachian riverscape brook trout movement in response to temperature flow, and thermal refugia within a compl. Trans. Am. Fish. Soc. 141, 1060–1073.
Plummer, L.N., Busenberg, E., Bohlke, J.K., Nelms, D.L., Michel, R.L., Schlosser, P., 2001. Groundwater residence times in Shenandoah National Park, Blue Ridge Mountains, Virginia, USA: a multi-tracer approach. Chem. Geol. 179, 93–111.
Rosenberry, D.O., Briggs, M.A., Delin, G., Hare, D.K., 2016a. Combined use of thermal methods and seepage meters to efficiently locate quantify, and monitor focused groundwater discharge to a sand-bed stream. Water Resour. Res. 52, 4486–4503.
Rosenberry, D.O., Briggs, M.A., Voytek, E.B., Lane, J.W., 2016b. Influence of groundwater on distribution of dwarf wedgemussels (Alasmidonta heterodon) in the upper reaches of the Delaware river, northeastern USA. Hydrol. Earth Syst. Sci. 20, 1–17.
Snyder, B.C.D., Webb, J.R., Young, J.A., Johnson, Z.B., Jewell, S., USGS, 2013. Significance of headwater streams and perennial springs in ecological monitoring in Shenandoah National Park. Open File Rep. 2013–1178, 46.

Snyder, C.D., Hitt, N.P., Young, J.A., 2015. Accounting for groundwater in stream fish thermal habitat responses to climate change. Ecol. Appl. 00, 281–304.
Stonestrom, D.A., Constantz, J., 2003. Heat as a tool for studying the movement of ground water near streams. U.S. Geol. Surv. Circ. 1260 96, 1–6.
Taylor, C.J., Pedregal, D.J., Young, P.C., Tych, W., 2007. Environmental time series analysis and forecasting with the captain toolbox. Environ. Model. Softw. 22, 797–814.
Vogt, T., Schirmer, M., Cirpka, O.A., 2012. Investigating riparian groundwater flow close to a losing river using diurnal temperature oscillations at high vertical resolution. Hydrol. Earth Syst. Sci. 16, 473–487.
Voss, C.I., Provost, A.M., 2002. SUTRA: A Model for Saturated-Unsaturated, Variable-Density Ground-Water Flow with Solute or Energy Transport. U.S. Geol. Surv. Water Resour. Invest. Rep. 02-4231, Reston, VA.
Waples, D.W., Waples, J.S., 2004. A review and evaluation of specific heat capacities of rocks, minerals, and subsurface fluids. Part 2: fluids and porous rocks. Nat. Resour. Res. 13, 123–130.
Ward, A.S., Gooseff, M.N., Singha, K., 2010. Characterizing hyporheic transport processes—interpretation of electrical geophysical data in coupled stream–hyporheic zone systems during solute tracer studies. Adv. Water Resour. 33, 1320–1330.
Wehrly, K., Wang, L., Mitro, M., 2007. Field-based estimates of thermal tolerance limits for trout: incorporating exposure time and temperature fluctuation. Trans. Am. Fish. Soc. 136, 365–374.
Yanamaka, H., Takemura, M., Ishida, H., Niwa, M., 1994. Characteristics of long-period microtremors and their applicability in exploration of deep sedimentary layers. Bull. Seismol. Soc. Am. 84, 1831–1841.